Electronic and Electrochemical Properties of $Li_xNi_{1-y}Co_yO_2$ Cathodes Studied by Impedance Spectroscopy

F. Nobili,[†] F. Croce,[‡] B. Scrosati,[‡] and R. Marassi*,[†]

Dipartimento di Scienze Chimiche, Università di Camerino, 62032, Camerino, Italy, and Dipartimento di Chimica, Università di Roma "La Sapienza", 00185, Roma, Italy

Received July 25, 2000. Revised Manuscript Received February 6, 2001

An electrochemical impedance spectroscopy (EIS) study of three members of the family of compounds $Li_xNi_{1-y}Co_yO_2$ ($y = 0$, 0.2, and 1) has been performed by taking spectra at closely spaced bias potentials over the potential windows of utilization as cathodes in lithium-ion batteries. The spectra have been interpreted in terms of electronic and ionic transport properties. It has been found that, for x values greater than about 0.9, all the compounds show semiconductive properties with a specific resistance that increases with decreasing Ni content. For x close to about 0.9−0.8, the properties change into those of a metal-like material in which the ionic conductivity becomes the limiting factor. The transition between these two limiting conditions clearly appears in the impedance spectra.

Introduction

Several experimental and theoretical papers[1−16] have established a correlation between the electronic structure, the type of discharge curve, and the electrical characteristics in compounds of the type A_xMX_2 (A = Li, Na; M = V, Cr, Mn, Co, Ni; X = O, S, Se) that find use as cathodes in Li-ion batteries. According to Goodenough[17] and Molenda,[2] who developed a band theory to explain the experimental findings, A_xMX_2-type compounds may be classified in two categories on the basis of the R_{M-M} distance in the crystal lattice. When R_{M-M} is greater than the critical value R_c, the system is an insulator and presents a steplike discharge curve. Systems with $R_{M-M} < R_c$ are correlated metals with a monotonic discharge profile. The conductivity in the first type of compounds is thermally activated.[1−3,14,18] For A_xMO_2 oxides in octahedral coordination the critical R_c values (corresponding to the "*a*" parameter of the cell) may be computed using a formula given in ref 17. In compounds such as Li_xCoO_2, Li_xNiO_2, and mixed oxides such as $Li_xNi_{1-y}Co_yO_2$, the R_{M-M} distance crosses the critical R_c value during the early stage of deintercalation. Thus, a semiconductor to metal transition is observed. This has been demonstrated in the case of Li_xCoO_2, by in situ conductivity measurements[5] and has been proposed to be responsible for the occurrence of the two-phase region appearing upon Li deintercalation.[9,14] The transition occurs in the x range from 1 to about 0.9 with an increase of more than 3 orders of magnitude in conductivity.

The literature data leave no doubts about the existence of a drastic variation of the electrical conductivity upon lithium deintercalation in this type of materials. A detailed discussion is the aim of this work where we want to demonstrate that (i) the conductivity change in this family of compounds must necessarily be reflected in the ac-impedance dispersion and (ii) a correct interpretation of the ac-impedance dispersions at different degrees of intercalation must include an element in the equivalent circuit that takes into account this variation. In a recent paper[4] we demonstrated the possibility of interpreting the evolution of the ac-impedance spectra of $Li_xNi_{0.75}Co_{0.25}O_2$, taking into account the intrinsic electronic resistance of the material. The results obtained showed that it is indeed possible to use EIS as a relatively simple, but powerful

* To whom correspondence should be addressed. Tel.: (39)-0737-402214. E-mail: marassi@camserv.unicam.it.
[†] Università di Camerino.
[‡] Università di Roma "La Sapienza".

(1) Molenda, A.; Stopklosa, T. Bak, *Solid State Ionics* **1989**, *36*, 53.
(2) Molenda, J. *Phys. Status Solid (b)* **1989**, *165*, 419.
(3) Molenda, J.; Wilk, P.; Marzec, J. *Solid State Ionics* **1999**, *119*, 19.
(4) Croce, F.; Nobili, F.; Deptula, A.; Lada, W.; Tossici, R.; D'Epifanio, A.; Scrosati, B.; Marassi, R. *Electrochem. Commun.* **1999**, *1*, 605.
(5) Shibuya, M.; Nishina, T.; Matsue, T.; Uchida, I. *J. Electrochem. Soc.* **1996**, *143*, 3157.
(6) Sato, H.; Takahaschi, D.; Nishima, T.; Uchida, I. *J. Power Sources* **1997**, *68*, 540.
(7) Cho, J.; Jung, H.; Park, Y. C.; Kim, G. B.; Lim, H. S. *J. Electrochem. Soc.* **2000**, *147*, 15.
(8) Aydinol, M. K.; Kohan, A. F.; Ceder, G.; Cho, K.; Joannopoulos, J. *Phys. Rev. B* **1997**, *56*, 1354.
(9) Van der Ven, A.; Aydinol, M. K.; Ceder, G.; Kresse, G.; Hafner, J. *Phys. Rev. B* **1998**, *58* (6), 2975.
(10) Van der Ven, A.; Aydinol, M. K.; Ceder, G. *J. Electrochem. Soc.* **1998**, *145*, 2149.
(11) Koyama, Y.; Kim, Y. S.; Tanaka, I.; Adachi, H. *Jpn. J. Appl. Phys.* **1999**, *38*, 2024.
(12) Koyama, Y.; Tanaka, I.; Kim, Y. S.; Nishitani, S. R.; Adachi, H. *Jpn. J. Appl. Phys.* **1999**, *38*, 4804.
(13) Montoro, I. A.; Abbate, M.; Rosolen, J. M. *Electrochem. Solid State Lett.* **2000**, *3*, 410.
(14) Ménétrier, M.; Saadoune, I.; Levassaur, S.; Delmas, C. *J. Mater. Chem.* **1999**, *9*, 1135.
(15) Carewska, M.; Scaccia, S.; Croce, F.; Arumugam, S.; Wang, Y.; Greenbaum, S. *Solid State Ionics* **1997**, *93*, 227.
(16) Tukamoto, H.; West, A. R. *J. Electrochem. Soc.* **1997**, *144* (9), 3164.
(17) Goodenough, J. B. *Solid. State. Chem.* **1971**, *5*, 279.
(18) Croce, F.; Nobili, F.; Tossici, R.; Scrosati, B.; Persi, L.; Marassi, R. Paper No. 239, IMLB 2000, Como, Italy, 2000.

10.1021/cm000600x CCC: $20.00
Published on Web 04/28/2001

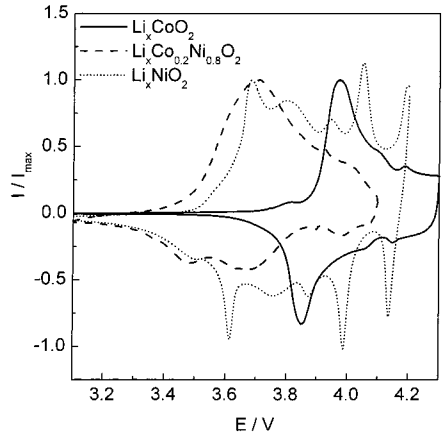

Figure 1. Steady-state cyclic voltammograms for all the studied compounds. Scan rate 10 μV s^{-1}. Each curve has been normalized to the maximum current of the main anodic wave.

tool for measuring the relevant parameters relative to the transport properties of these intercalation materials. In this paper we extend our study to other members of the same family, namely, Li_xCoO_2, Li_xNiO_2, and $Li_xNi_{0.8}Co_{0.2}O_2$.

Experimental Section

The compounds used during this study ($LiCoO_2$, $LiNiO_2$, and $LiNi_{0.8}Co_{0.2}O_2$) were Merck, battery grade. The electrodes were prepared by spraying a dispersion of each compound—poly(vinyl chloride) (PVC, high molecular weight, Fluka) acetylene black carbon (90:5:5 w/o) in tetrahydrofuran (HPLC grade, Carlo Erba)—on a 10-μm-thick high-purity Al foil. The electrodes were dried at 80 °C under vacuum for at least 24 h before being inserted into the electrochemical cell. Typical loadings of the electrodes were between 1 and 2 mg/cm^2 of active material. The cell was a T-shaped polyethylene Swagelok-type cell equipped with stainless steel (SS304) current collectors. Disks of Foote high-purity lithium foil were used as counter and reference electrodes, respectively. The electrolyte was a 1 M $LiClO_4$ ethylene carbonate−dimethyl carbonate (EC−DMC 1:1, Merck battery grade). A microporous polypropylene film (Celgard 3501, Celanese Co.) was used as a separator. The cells were assembled into an argon-filled drybox with a moisture and oxygen level below 2 ppm. The cells were generally cycled at least one time at a slow scan rate in the box and sealed afterward. This permitted the elimination of any gaseous product formed during the formation of the solid electrolyte interface (SEI) on the electrodes. The sealed cells were tested outside the drybox using a silicon oil bath to regulate the experimental temperature. Unless otherwise stated, all the experiments were run at 20 °C. All the electrochemical measurements were performed using a CH650 electrochemical station (Cordova, TN) driven by a PC. The impedance spectra were taken in the frequency range 1 mHz to 100 kHz. The instrument was driven by a macro routine that included a series of potentiostatic steps each followed by the impedance measurement. The time window of the potentiostatic steps was regulated in such a way to ensure that equilibrium conditions were reached. The required times were of the order of several hours, depending on the extent of the potential change (generally 10 mV) from the previously acquired bias potential.

Results and Discussion

Figure 1 shows typical low scan rate steady-state cyclic voltammograms for the three different compounds traced at 10 μV s^{-1}. Because of the very low scan rate, the curves reflect a quasi-equilibrium condition and, thus, have been used, after integration, to obtain a quasi-thermodynamic x versus E curves. These were used to assign a given intercalation degree x to a given electrode potential of the Li/$Li_xNi_{1-y}Co_yO_2$ cells.

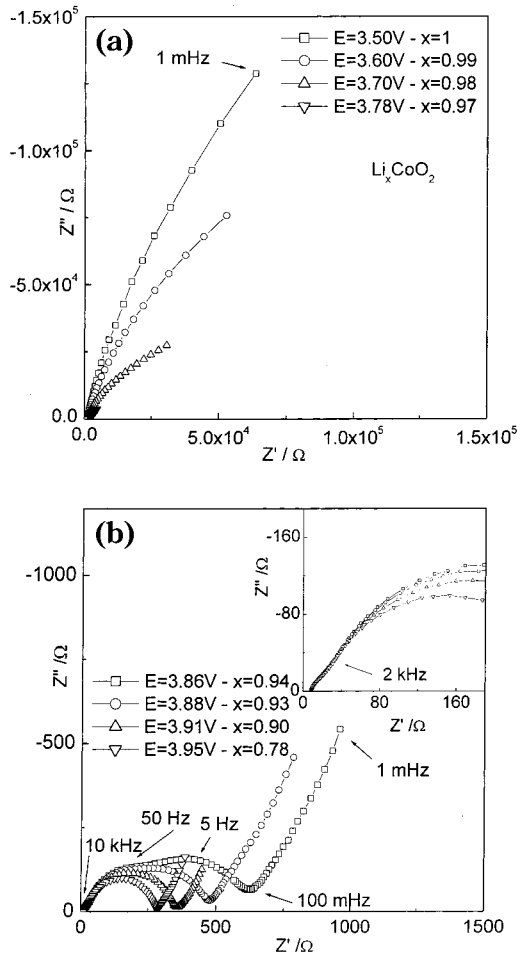

Figure 2. Nyquist plots taken at different potentials for the compound Li_xCoO_2. Frequency range, 1 mHz to 100 kHz.

Figures 2−4 show some Nyquist plots measured at different potentials for the three different compounds. Panels (a) in all figures show the dispersions obtained at potentials at the foot of the deintercalation peak when the lithium content is close to 1. Panels (b) show the spectra obtained at lower x values. The inserts in the panels (b) show magnification of the high-frequency region. A common feature of all dispersions is a high-frequency, more or less defined, semicircle indicative of the presence of a passivating layer. A comparison of panels (a) and (b) shows that the impedance response is largely potential dependent. First of all, the impedance drastically decreases with decreasing x. At high x values the dispersions are dominated by a low-frequency semicircle that shows an increasing tendency to close on the real axis as the voltage increases. In previous work[19,20] on this type of compound, the high impedance values at high x have been attributed to a capacitive behavior and/or to an extremely high value of the charge-transfer resistance R_{ct}. However, the frequency range (<1 Hz) appears too low for a charge transfer process. This, together with the fact that at potentials

(19) Levi, M. D.; Salitra, G.; Marcowsky, B.; Teller, H.; Aurbach, D.; Eider, U.; Eider, L. *J. Electrochem. Soc.* **1999**, *146*, 1279.
(20) Levi, M. D.; Gamolsky, K.; Aurbach, D.; Eider, U.; Oesten, R. *Electrochim. Acta* **2000**, *45*, 1781.

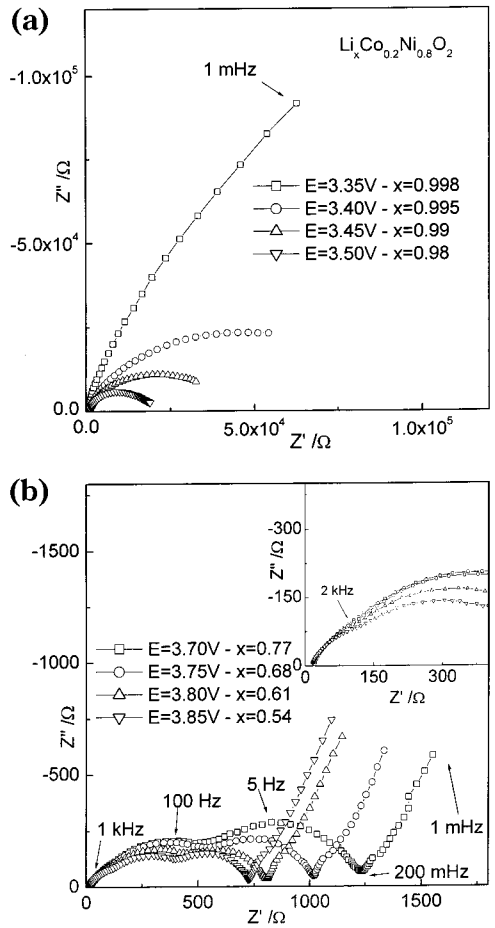

Figure 3. Nyquist plots taken at different potentials for the compound $Li_xNi_{0.8}Co_{0.2}O_2$. Frequency range, 1 mHz to 100 kHz.

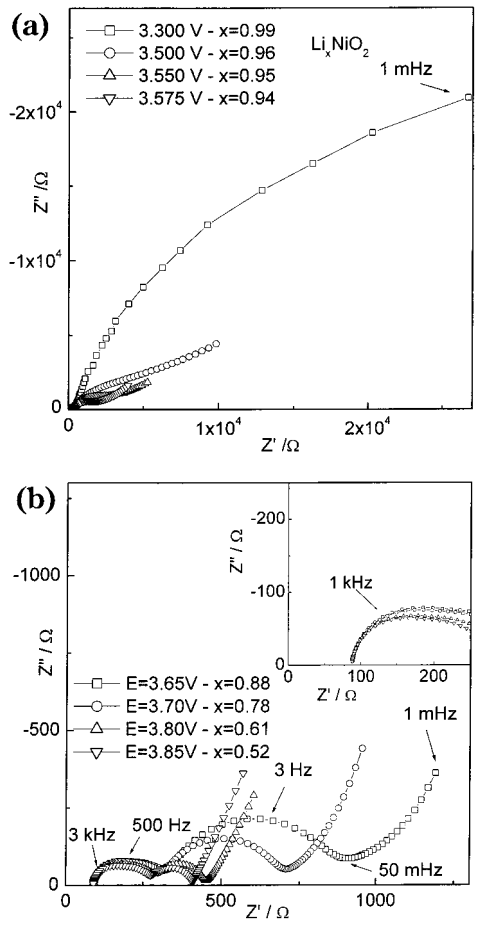

Figure 4. Nyquist plots taken at different potentials for the compound Li_xNiO_2. Frequency range, 1 mHz to 100 kHz.

corresponding to the beginning of the deintercalation peak a more or less defined, depending on the type of compound, third semicircle becomes increasingly evident in the frequency range from 10 Hz to 1 kHz, may lead to a different interpretation: that is, the high impedance and the potential dependence of the low-frequency semicircle may be attributed to the variation of the electronic conductivity of the material, while charge transfer can be associated with the middle-frequency semicircle. This interpretation is supported by several facts. First of all, the interface between the current collector and the active material is blocking for Li ions. If this is true, one would expect, in the absence of a charge transfer process, the imaginary part of Z to tend to infinity as the frequency tends to zero. The fact that the semicircle tends to close or closes on the real axis at almost any potential appears to be reasonably explained by a change of the electronic conductivity. This assumption is supported by a variety of literature data that demonstrate that each one of the studied materials undergoes an insulator to metal transition.

In the spectra at higher potentials (lower x), the low-frequency limit (1 mHz) starts to show the characteristic spike associated with the well-known thin-layer ionic diffusion. To summarize, it appears that, as was the case for $Li_xNi_{0.75}Co_{0.25}O_2$,[4] the evolution of the dispersions may be described as associated with all the physical phenomena that characterize a charge transfer at passivated materials, that is, (i) a high-frequency dispersion (<1 kHz) characteristic of a SEI passivating

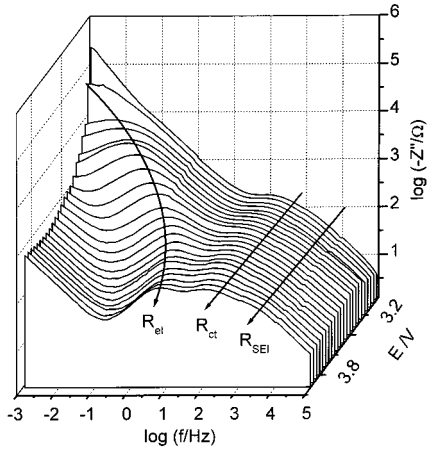

Figure 5. Frequency dependence of impedance (imaginary part) of $Li_xNi_{0.8}Co_{0.2}O_2$. The arrows indicate the potential dependence of the different physical phenomena.

layer; (ii) an intermediate-frequency dispersion (between 10 Hz and 1 kHz) characteristic of a charge transfer process; (iii) a well-developed low-frequency semicircle associated with the electronic properties of the material, and finally (iv) the very low frequency spike of the ionic diffusion.

The potential dependence of the different spectral features that may be associated with the different physical phenomena is fairly well illustrated in Figure 5 by the Bode plots of the imaginary part of the impedance relative to $Li_xNi_{0.8}CO_{0.2}O_2$. As may be seen,

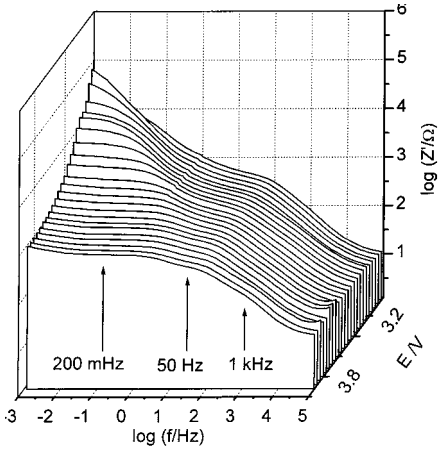

Figure 6. Frequency dependence of impedance (real part) of $Li_xNi_{0.8}Co_{0.2}O_2$. The arrows indicate the frequency region of interest of the different physical phenomena.

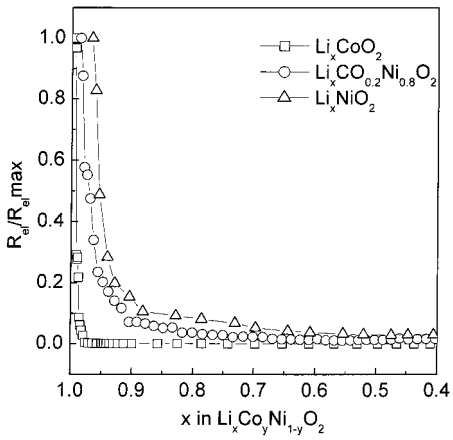

Figure 7. Normalized electronic resistance at different x values.

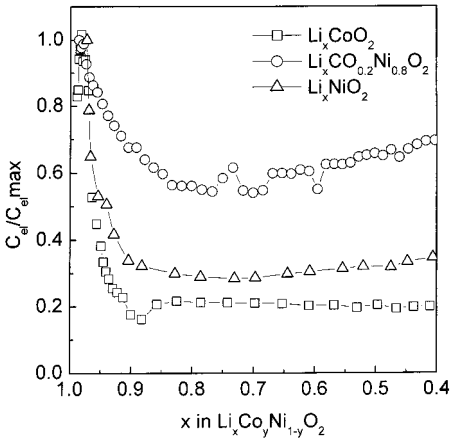

Figure 8. Normalized capacitance associated with the electronic resistance at different x values.

several peaks may be identified. Each one of them corresponds to the radius of a semicircle in the corresponding Nyquist plot. The arrows in the figure approximately indicate how the frequency changes with potential. It is clear that while the radius of the low-frequency semicircle is potential dependent, the other two, SEI, at the high-frequency limit, and R_{ct}, in the middle-frequency range, are practically invariant with potential. On the basis of the previous considerations, the low-frequency peak may be assigned to the resistance of the material that changes about 3 orders of magnitude for a variation of x from about 1 to 0.9. The same type of information may be obtained from Figure 6 relative to the real part of the impedance. The high-frequency limit of the $Z_{[Re]}$ is potential independent and constant. This means that the solution resistance is constant. The plateau at the low-frequency limit, corresponding to the intersection with the real axis of the semicircle assigned to the electronic resistance of the material, is clearly potential dependent, as was the case for the equivalent peak in Figure 5. A similar analysis of the Bode plots for $LiCoO_2$ has been published by Sato et al.[6] In their case the interpretation was simpler because the electrode was very thin and the spectra could be interpreted on the basis of a simple Randles circuit that included only the solution resistance in series with a capacity parallel to a Warburg element and the film resistance.

Bode plots for the other two compounds are quite similar to those shown for $Li_xNi_{0.8}CO_{0.2}O_2$. The only differences lie in the separation of the different semicircles. In the case of $LiCoO_2$, for x values below 0.94, the time constants for R_{ct} and R_e, and hence the peaks in the corresponding plots of the imaginary part of the impedance vs frequency, are close (0.05 and 0.003 s, respectively, see Figure 2b). The difference in the time constant values becomes more and more pronounced at lower temperatures.[18,21]

As has been done in a previous paper, the EIS data have been fitted using an equivalent circuit similar to that reported by Levi and co-workers[19] for $LiCoO_2$.The circuit includes the solution resistance, three RQ elements (where Q is the general element defined in ref 22), a Warburg element, and capacitor corresponding to the intercalation capacity. In order of decreasing frequency range, the three RQ elements represent the SEI, R_{ct}, and the film resistance. The spectra have been fitted using the Boukamp program.[22]

A detailed discussion of all the features and relevant parameters, with special emphasis on their temperature dependence, of the EIS study relative to the different compounds are at present in preparation.[21] Here, we will limit our discussion to the RQ element associated with the electronic resistance of the electrodic material. Figures7 and 8 show the plots of R_e and of the associated capacity, (Q) vs x. To compare the behavior of the three different compounds, both parameters have been normalized to the respective values measured at 3.5 V. At this potential the intercalation degrees, as determined from the slow rate cyclic voltammograms, are 1, 0.98, and 0.96 respectively for Li_xCoO_2, $Li_xNi_{0.8}CO_{0.2}O_2$, and Li_xNiO_2. It is clear that the resistances drop drastically over a very narrow potential range corresponding approximately to x values between 1 and $\cong$0.8. The absolute values used for normalization, as deduced from

(21) Nobili, F.; Croce, F.; Scrosati, B.; Marassi, R., in preparation

(22) Boukamp, B. A. *Solid State Ionics* **1986**, *20*, 159.
(23) Granqvist, C. G. *Appl. Physi. A* **1993**, *57*, 3.

the simulation, are of the order of 0.84 MΩ, 21 kΩ, and 2 kΩ for Li_xCoO_2, $Li_xNi_{0.8}CO_{0.2}O_2$, and Li_xNiO_2, respectively. Although only indicative because of the differences in the electrode characteristics (texture, porosity, grain size, etc.), the values are consistent with those of the specific resistivity for the three compounds at room temperature as deduced from the graphs in Molenda's papers[1,3] (5 kΩ cm, 6 Ω cm, and 0.4 Ω cm, respectively) and with the conclusion that an increase of the Ni content leads to a decrease of the semiconductor properties of these materials. As may be seen from Figure 8, the capacities follow the same trends of the respective resistances. A possible physical explanation of the capacities is the formation of capacitors due to accumulation of electrons at the surface of the nanocrystallites forming the particles due to difficult electron flow.[23] The measured absolute values of this parameter, related to the particles morphology, are quite close and in the range of hundreds of μF.

Conclusions

The results obtained in this EIS study confirm those already published[4] in the case of $LiNi_{0.75}Co_{0.25}O_2$. At the initial stages of lithium deintercalation the EIS spectra are dominated by the electronic conductivity of the materials that undergo a semiconductor to metal transition for x values around 0.9−0.8. Consideration of the presence of this conductivity change seems to be essential for a correct interpretation of the impedance dispersions. EIS has been demonstrated to be a simple but powerful tool for measuring the relevant transport parameters that are very important in defining the practical usability of a material such as an intercalation electrode.

Financial support from MPI and Consiglio Nazionale delle Ricerche, Progetto Finalizzato Materiali Avanzati II, Contributo 99.01820.Pf.34 is acknowledged.

CM000600X